European Journal of Radiology 120 (2019) 108687

Contents lists available at ScienceDirect

European Journal of Radiology

journal homepage: www.elsevier.com/locate/ejrad

Research article

Direct evaluation of peripheral airways using ultra-high-resolution CT in chronic obstructive pulmonary disease

Naoya Tanabe[a,*], Hiroshi Shima[a], Susumu Sato[a], Tsuyoshi Oguma[a], Takeshi Kubo[b], Satoshi Kozawa[c], Koji Koizumi[c], Atsuyasu Sato[a], Kaori Togashi[b], Toyohiro Hirai[a]

[a] Department of Respiratory Medicine, Graduate School of Medicine, Kyoto University, 54 Kawahara-cho, Shogoin, Sakyo-ku, Kyoto 606-8507, Japan
[b] Department of Diagnostic Imaging and Nuclear Medicine, Graduate School of Medicine, 54 Kawahara-cho, Shogoin, Sakyo-ku, Kyoto 606-8507, Japan
[c] Division of Clinical Radiology Service, Kyoto University Hospital, 54 Kawahara-cho, Shogoin, Sakyo-ku, Kyoto 606-8507, Japan

ARTICLE INFO

Keywords:
Computed tomography
Lung
Small airway
Chronic obstructive pulmonary disease
Emphysema

ABSTRACT

Purpose: Disease in small airways < 2 mm in diameter is a major pathology of chronic obstructive pulmonary disease (COPD). However, compared to airways < 1 mm in diameter, the pathophysiological role of airways 1–2 mm in diameter remains unclear. This study analysed phantom and human COPD data to test the hypothesis that ultra-high-resolution computed tomography (U-HRCT) can accurately measure peripheral airways that are difficult to measure with conventional CT.

Method: The lower limit of lumen sizes measurable on U-HRCT was determined using phantom tubes. In the cross-sectional data of 110 males with COPD who underwent U-HRCT (1024 × 1024 matrix, 0.25 mm slice thickness) and spirometry, all 3rd (segmental) to 6th generation airways of the right apical and basal posterior bronchus (RB1 and RB10) were analysed.

Results: The errors in measuring the lumen area (LA) of phantom tubes ≥1.3 and 1.0 mm in diameter were within ± 10 and -24%, respectively. The internal diameters for 70 and 62% of the 6th generation RB1 and RB10 airways were < 2 mm. The numbers of 6th generation RB1 and RB10 airways decreased as the airflow limitation severity increased. Among the mean LA and sum of LA(sum-LA) of the 3rd to 6th generation airways, the sum-LA of the 6th generation had the largest impact on airflow limitation.

Conclusions: U-HRCT enables accurate and direct evaluation of peripheral airways 1–2 mm in diameter. The 6th generation airways are commonly < 2 mm in diameter, and the sum-LA can be a useful CT biomarker that reflects airflow limitation in COPD.

1. Introduction

Chronic obstructive pulmonary disease (COPD) is a leading cause of death worldwide [1]. COPD is physiologically characterized by chronic airflow limitation that is closely associated with two pathological changes: emphysema and disease of the small airways, which are generally defined as bronchioles < 2 mm in diameter [2]. While studies using histology and micro-computed tomography have intensively investigated small airways < 1 mm in diameter, including the preterminal and terminal bronchioles, and have shown pathogenetic interactions between disease in these airways and emphysema [3–7], much remains to be elucidated about the pathophysiological role of small airways 1–2 mm in diameter in COPD.

Currently, standard computed tomography (CT) (512 × 512 matrix and ≥0.5 mm slice thickness) is used to measure the dimensions of central airways, such as the 3rd (segmental) and 4th generation airways [8–12]. Several studies have attempted quantitative measurements of the 5th and 6th generation airways [13–15], but these measurements

Abbreviations: COPD, chronic obstructive pulmonary disease; CT, computed tomography; $CTDI_{vol}$, volume CT dose index; FEV_1, forced expiratory volume in 1 s; FIRST, the forward-projected model-based iterative reconstruction solution; FVC, forced vital capacity; HU, Hounsfield units; ID, internal diameter; LAV%, low attenuation volume percent; LA, lumen area; Mean-LA, mean luminal area; $\%FEV_1$, percent forced expiratory volume in 1 s; RB1, right apical segment; RB10, right posterior basal segment; Sum-LA, sum of lumen areas; U-HRCT, ultra-high-resolution computed tomography

* Corresponding author at: Department of Respiratory Medicine, Graduate School of Medicine, Kyoto University, 54 Kawahara-cho, Shogoin, Sakyo-ku, Kyoto 606-8507, Japan.

E-mail addresses: ntana@kuhp.kyoto-u.ac.jp (N. Tanabe), hirocima2469@kuhp.kyoto-u.ac.jp (H. Shima), ssato@kuhp.kyoto-u.ac.jp (S. Sato), toguma@kuhp.kyoto-u.ac.jp (T. Oguma), tkubo@kuhp.kyoto-u.ac.jp (T. Kubo), kozawa@kuhp.kyoto-u.ac.jp (S. Kozawa), koiz@kuhp.kyoto-u.ac.jp (K. Koizumi), atsuyasu@kuhp.kyoto-u.ac.jp (A. Sato), ktogashi@kuhp.kyoto-u.ac.jp (K. Togashi), t_hirai@kuhp.kyoto-u.ac.jp (T. Hirai).

https://doi.org/10.1016/j.ejrad.2019.108687
Received 12 July 2019; Received in revised form 4 September 2019; Accepted 17 September 2019

might include potential bias from the limited image resolution. Indeed, even the visibility of the 5th and 6th generation airways is impaired in COPD [16], and spatially matched comparisons of their sizes is challenging [11]. Moreover, the finding of impaired airway visibility suggests that the 5th and 6th generation airways in COPD may include airways < 2 mm in diameter, which is below the lower limit of quantitation for standard CT with a 512 × 512 matrix [10,13,17].

The recently introduced and commercially available technology of ultra-high-resolution CT (U-HRCT) acquires images of live persons with a 1024 × 1024 matrix and 0.25 mm slice thickness without increases in radiation dose and allows for clearer visualization of organ structure such as lung than conventional CT [18–20]. In addition, a phantom study showed that the lumen size of a tube 2 mm in diameter could be accurately quantified using U-HRCT [17]. Therefore, the lower limit of lumen size quantitation for airways < 2 mm in diameter on U-HRCT needs to be established.

We hypothesized that U-HRCT allows for the accurate and direct evaluation of peripheral airways 1–2 mm in diameter and provides unbiased information regarding their clinical and physiological impacts in COPD. The aim of this study was to examine whether the lumen size of phantom tubes < 2 mm in diameter could be accurately quantified with U-HRCT. We also aimed to analyse all the 3rd to 6th generation airways to test whether the 5th and 6th generation airways in COPD were commonly < 2 mm in diameter and whether the assessment of luminal narrowing in these airways using U-HRCT is closely associated with airflow limitation in COPD.

2. Material and methods

2.1. Patient enrolment and ethics statement

This is a retrospective cross-sectional study using clinical data from consecutive patients with COPD who underwent inspiratory chest U-HRCT and spirometry in our hospital during an exacerbation-free period between February 2018 and January 2019. U-HRCT images were obtained using an Aquilion Precision scanner (Cannon Medical Systems, Otawara, Japan) that has been commercially available since 2017. The inclusion criteria were a smoking history of at least 20 pack-years and a diagnosis of COPD confirmed by post-bronchodilator forced expired volume in 1 s (FEV_1)/forced vital capacity (FVC) ratio < 70% [21]. The exclusion criteria were alpha-1 antitrypsin deficiency, other lung diseases such as interstitial pneumonia, atelectasis, and bronchiectasis, and a prior history of surgical lung resection. The study was approved by the ethics committee of our institution (approval No. R1660), and informed consent was waived due to the retrospective use of the data.

2.2. Phantom

The custom-made airway phantom included 8 tubes of different sizes that were placed in a circle and embedded in urethane foam. The largest tubes (3 mm internal diameter and 0.7 mm wall thickness) were made of acrylic resin, and the other tubes ≤2 mm internal diameter were made of polyethylene. The details of the sizes of tubes are described in the online supplemental Figure A1.

2.3. CT scan

The airway phantom was imaged using ultra-high-resolution (Aquilion Precision) and conventional scanners (Aquilion ONE, Cannon Medical Systems, Otawara, Japan). The Aquilion Precision scanner generated 1024 × 1024 matrix images with 0.25 mm slice thickness using 0.25 × 0.25 mm detector elements in the super high-resolution (SHR) mode [17,18]. The Aquilion ONE scanner generated 512 × 512 matrix images with 0.5 mm slice thickness using 0.5 × 0.5 mm detector elements. The scanning conditions for both scanners were 120 kVp, 240 mA, 0.5 s exposure time, pitch factor of 0.81, and 350 mm field of view. The CT images were reconstructed using a full iterative reconstruction method, namely, the forward-projected model-based iterative reconstruction solution (FIRST) algorithm [22]. In the clinical study, all patients with COPD were scanned with the Aquilion Precision scanner using the same scanning parameters and auto-exposure control. In addition to 1024 × 1024 matrix images with 0.25 mm slice thickness (U-HRCT), conventional 512 × 512 matrix images with 0.5 mm slice thickness were reconstructed in 20 patients to compare airways visualized on U-HRCT to those on conventional CT. Radiation exposure was estimated using the volume CT dose index ($CTDI_{vol}$).

2.4. CT analyses

The phantom tubes and human airways were quantitatively analysed using SYNAPSE VINCENT software (FUJIFILM Medical, Tokyo, Japan). In the phantom tube analyses, the lumens of the phantom tubes were automatically segmented, and the lumen area of each tube was measured. The measurement error (%) was obtained based on the following formula: 100 × (CT measurement – actual value) / actual value.

In the airway analyses of patients with COPD, the segmental bronchus was defined as the 3rd generation airway. Following automatic luminal segmentation of airway tree, all branches of the 3rd to 6th generation airways in the right apical (RB1) and posterior basal (RB10) segments were manually identified by tracking from the 3rd to the 6th generation [23]. For each branch, cross-sectional images perpendicular to the longitudinal centre line of the lumen were generated, and the lumen areas and internal diameters in the middle third portion were automatically measured and averaged (Supplementary Figure A2). The mean lumen area (mean-LA) for each generation airway, sum of lumen areas (sum-LA) for each of the 4th, 5th, and 6th generations, and number of airways for each of the 5th and 6th generations were calculated in the RB1 and RB10 segments. To calculate the mean-LA and sum-LA, the phantom data regarding the lower limit of quantitation for measuring lumen area was used.

To assess the severity of emphysema, the lung field was segmented, and the percentage ratio of voxels < -950 Hounsfield unit (HU) to all the voxels in the lung was calculated as the low attenuation volume percent (LAV%) [24].

2.5. Pulmonary function test

Spirometry was performed after bronchodilator inhalation using a Chestac-8900 (Chest MI, Tokyo, Japan). The predicted FVC and predicted FEV_1 were calculated with the LMS method [25].

2.6. Statistical analysis

Statistical analyses were performed using R version 3.5.1 (R Foundation for Statistical Computing (36)). Data are expressed as the mean ± standard deviation (SD) unless otherwise indicated. A p-value less than 0.05 was considered statistically significant. The inter-observer variability in the number of 6th generation airways that were manually identified on U-HRCT was assessed by using the intraclass correlation coefficient and Bland-Altman plot [26,27]. Correlations between the CT measurements and pulmonary function were evaluated using the Pearson correlation tests. To explore the relative contributions of the airway measurements and emphysema to airflow limitation, multivariable linear regression models were constructed using $\%FEV_1$ as a dependent variable and LAV% and the airway measure in the RB1 and RB10 segments of each airway generation as independent variables.

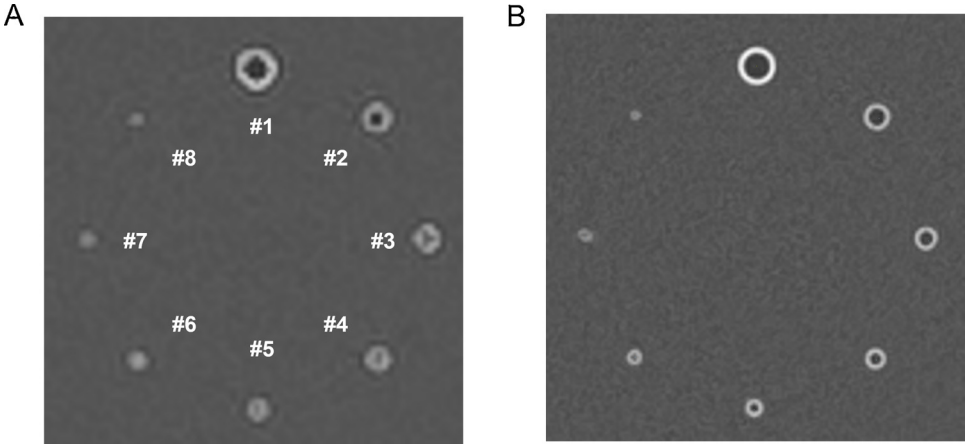

Fig. 1. Representative images of the phantom tubes with conventional and ultra-high-resolution CT. The internal diameters are as follows: [#1] 3.0 mm, [#2] 2.0 mm, [#3] 1.6 mm, [#4] 1.3 mm, [#5] 1.0 mm, [#6 and 7] 0.8 mm, and [#8] 0.5 mm. The wall thickness was 0.7 mm for tube [#1], 0.5 mm for tubes [#2-6], and 0.3 mm for tubes [#7 and 8]. (A) Conventional CT (512 × 512 pixel size and 0.5 mm slice thickness). (B) Ultra-high-resolution CT (U-HRCT, 1024 × 1024 pixel size and 0.25 mm slice thickness) for the same tubes, and the locations corresponded to those on the conventional CT. U-HRCT, but not conventional CT, clearly visualized the lumen of tubes 1.0–2.0 mm in diameter (#2-5).

3. Results

3.1. Phantom study

Fig. 1 shows representative images showing the phantom tube lumens. The lumens of tubes with internal diameters between 1 mm and 2 mm were clearly visualized with U-HRCT but not with conventional CT. The errors in the measurements of lumen areas are summarized in Table 1. The errors for tubes ≥1.3, 1.0, and ≤0.8 mm in diameter with U-HRCT were within ± 10%, -24%, and < -40%, respectively.

3.2. Human study

As shown in the patient flowchart (Fig. 2), of the consecutive 142 patients with COPD who underwent U-HRCT and spirometry during an exacerbation-free period in our hospital, 21 patients were excluded due to abnormal radiological findings from causes other than COPD, such as interstitial pneumonia, and 6 were excluded due to a history of lung resection. In addition, 5 female subjects were excluded based on previous reports that found sex differences in airway dimensions [28,29]. A total of 110 patients were included in the present analyses. Table 2 shows the demographics of these patients. The mean ± SD value for $CTDI_{vol}$ was 10.9 ± 3.0 mGy.

Fig. 3 shows an example of U-HRCT image of a patient with COPD. The 6th generation airways were commonly < 2 mm in diameter (Fig. 3C), and these airways were more clearly visualized on U-HRCT than conventional 512 × 512 images (Fig. 3D). The intraclass correlation coefficients of the number of the 6th generation RB1 and RB10 airways that were manually identified by two observers, were 0.86 and 0.82, respectively. The Bland-Altman plots (Supplementary Figure A3) also show that the inter-observer variability of the number of the 6th generation in RB1 and RB10 segments was small (bias = -0.2 and -0.4, respectively). The number of the 6th generation RB1 airways identifiable on U-HRCT was more than on conventional CT (Supplementary Figure A4). Fig. 4 shows the distributions of internal diameters for the 3rd, 4th, 5th and 6th generation airways of the RB1 and RB10 segments. The percentages of airways < 2 mm in diameter in the 3rd, 4th, 5th, and 6th generations were 0, 4, 31, and 70% in the RB1 segment and 0, 10, 36, and 62% in the RB10 segment, respectively.

Table 1
Errors in measuring the luminal areas of phantom tubes using conventional CT with a 512 × 512 matrix and ultra-high-resolution CT scans.

	Conventional CT	U-HRCT
Matrix size	512 × 512	1024 × 1024
Slice thickness	0.5 mm	0.25 mm
Error in measuring lumen area		
ID = 3.0 mm (WT = 0.7 mm)	−25%	9%
ID = 2.0 mm (WT = 0.5 mm)	−30%	−8%
ID = 1.6 mm (WT = 0.5 mm)	NA	−1%
ID = 1.3 mm (WT = 0.5 mm)	NA	−2%
ID = 1.0 mm (WT = 0.5 mm)	NA	−24%
ID = 0.8 mm (WT = 0.5 mm)	NA	−40%
ID = 0.8 mm (WT = 0.3 mm)	NA	−80%
ID = 0.5 mm (WT = 0.3 mm)	NA	NA

ID = internal diameter. WT = wall thickness. NA = not available.

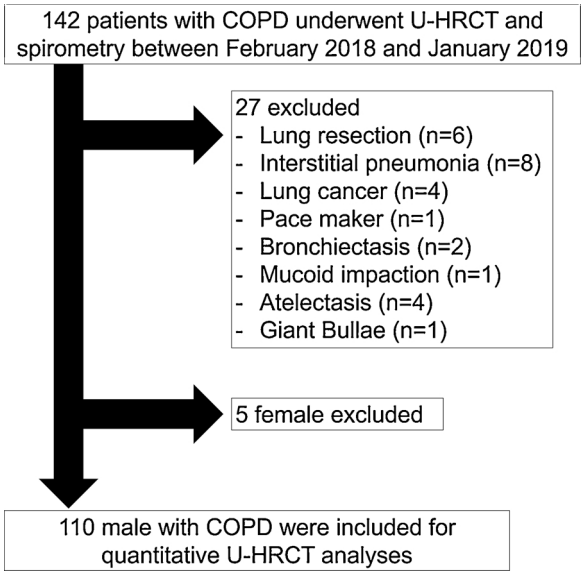

Fig. 2. Patient flowchart. U-HRCT = ultra-high-resolution computed tomography.

Table 2
Demographics of the study patients (n = 110).

Age	73 ± 8
Height (cm)	165 ± 6
Weight (kg)	64 ± 10
Smoking history (former/current)	81/29
Pack-Years	64 ± 35
FEV_1 (L)	1.79 ± 0.66
FEV (% of predicted)	67 ± 23
FVC (L)	3.38 ± 0.86
FEV_1/FVC (%)	52 ± 13
LAV% (%)	31 ± 12

All patients were male. Data are expressed as the mean ± SD. FEV_1 = forced expiratory volume in 1 s. FVC = forced vital capacity. LAV% = low attenuation volume percent.

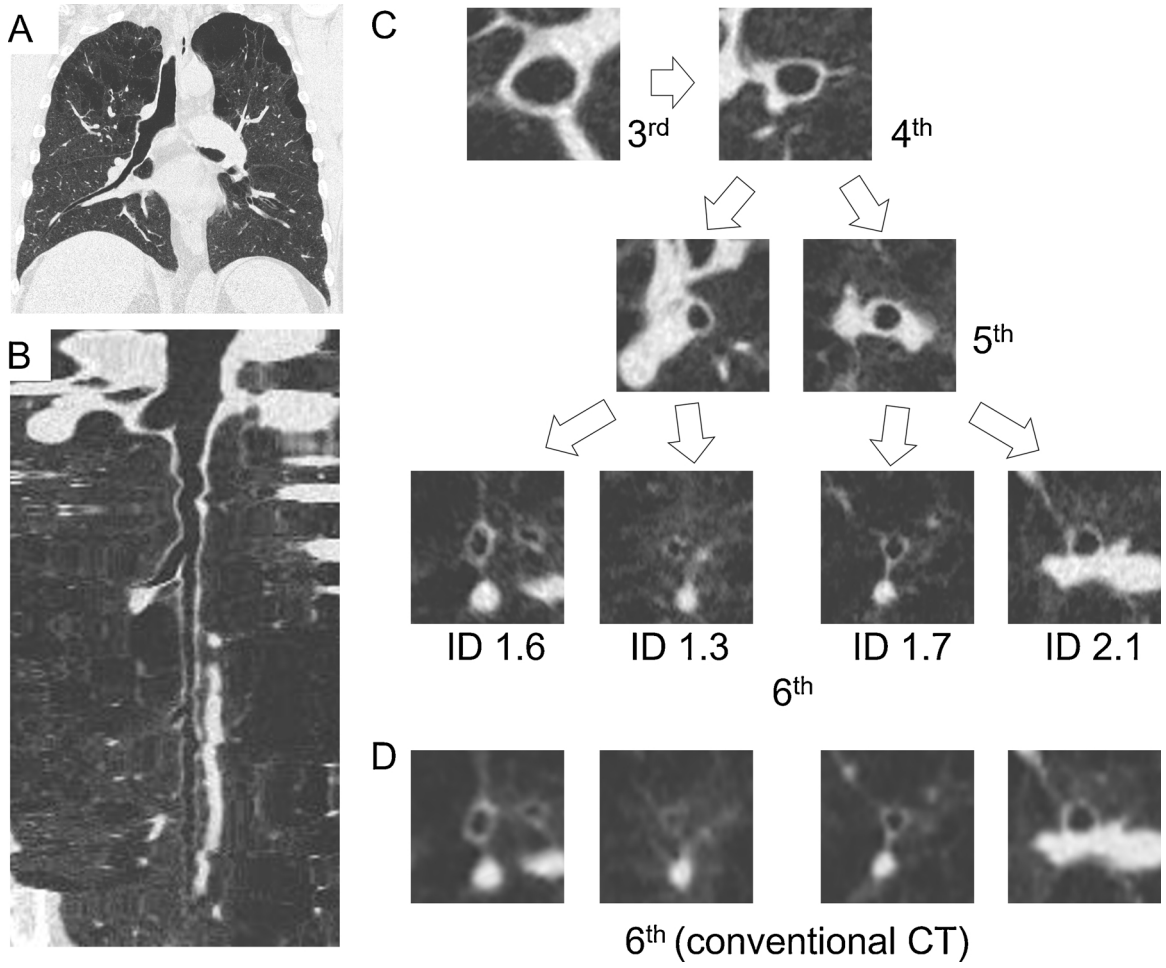

Fig. 3. Examples of ultra-high-resolution CT scans showing the lumens of the 3rd to 6th generation airways in a patient with COPD. (A) An airway tree was extracted from the original ultra-high-resolution CT (U-HRCT) scan. (B) Multiplanar reconstruction was performed along the centre line of the extracted airway tree. (C) All airways located at the 3rd to 6th generations of the right apical and basal posterior bronchus (RB1 and RB10) were evaluated, and their lumen sizes were quantified. (D) Compared to the 6th generation airways on U-HRCT, these airways were less clearly visualized on conventional 512 × 512 CT with 0.5 mm slice thickness. ID = internal diameter (mm).

Based on the phantom data (Fig. 1 and Table 1), the mean-LA and sum-LA were calculated from the data of all the airways > 1 mm in diameter. Table 3 summarizes the associations of the mean-LA and sum-LA and number of airways for each of RB1 and RB10 segments with %FEV_1. Fig. 5 shows that the correlation between sum-LA and %FEV_1 was greater in the 6th generation than in the 5th generation (RB1: r = 0.45 vs 0.32 and RB10: r = 0.36 vs 0.31). Supplementary Table A1 shows that the associations of sum-LA in the 6th generation of RB1 and RB10 segments with %FEV_1 were still found even after adjusting for the sum-LA by body surface area. Supplementary Table A2 shows that there was close correlation between the sum-LA of the 6th generation airways in both RB1 and RB10 segments and FEV_1/FVC.

Table 4 shows the results of the multivariable linear regression analyses. The sum-LA of the 6th generation airways in both the RB1 and RB10 segments were associated with %FEV_1 independent of LAV%.

4. Discussion

In this study, the phantom tube analyses provided evidence that airways 1–2 mm in diameter could be accurately quantified by U-HRCT but not by conventional CT. Furthermore, the airway analyses for patients with COPD showed that the 6th generation airways were commonly < 2 mm in diameter and that airflow limitation was more closely associated with the sum-LA of the 6th generation airways than with the sum-LA of the 4th and 5th generation airways and with the mean-LA of airways of any generation.

This is the first study to provide evidence that U-HRCT with a 1024 × 1024 matrix and 0.25 mm slice thickness enables the accurate and direct evaluation of peripheral airways 1–2 mm in diameter. Indeed, the U-HRCT provided better visualization of the 6th generation airways and allowed identifying the 6th generation airways more sufficiently than conventional 512 × 512 CT. In addition, an advantage of this study is the evaluation of all 3rd to 6th generation RB1 and RB10 airways to minimize sampling bias within each segment. Strikingly, 70 and 62% of the 6th generation airways in the RB1 and RB10 segments were < 2 mm in diameter, indicating that conventional CT is not appropriate to quantitatively measure the 6th generation airways. In contrast, computer-based quantitation of small airways 1–2 mm in diameter using U-HRCT has the potential to improve clinical management for patients with COPD. We postulate that this new modality can uncover longitudinal progression of peripheral airway disease in relation to progressive emphysema and can allow for sensitive detection of pharmacological effects that cannot be readily evaluated by conventional CT examinations of the central airways.

The number of the 6th generation airways of the RB1 and RB10 segments decreased as the %FEV_1 decreased (r = 0.27 and 0.33, respectively). This result extends upon previous findings that the total airway count with conventional CT decreases as the severity of COPD increases [4,16,30], and the number of terminal bronchioles on micro-computed tomography decreases in COPD compared to that in controls

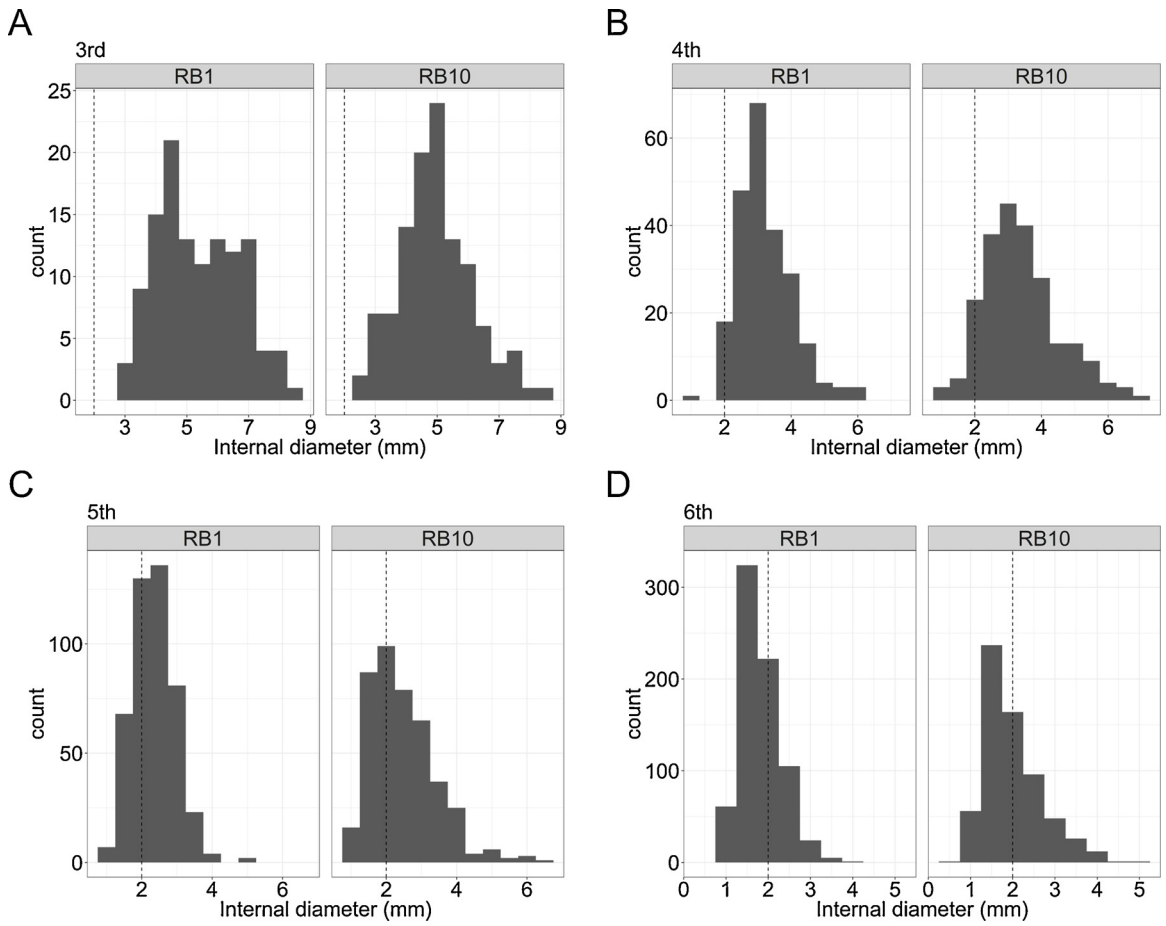

Fig. 4. Histogram of the internal diameters of the 3rd to 6th generation airways. Distributions of the internal diameters for the 3rd (A), 4th (B), 5th (C), and 6th (D) generation airways. The 3rd generation = segmental bronchus. RB1 and RB10 indicate the right apical and basal posterior segments, respectively. The dashed lines indicate an internal diameter of 2 mm. The percentages of airways < 2 mm in diameter for the 3rd, 4th, 5th, and 6th generations were 0, 4, 31, and 70% in the RB1 segment and 0, 10, 36, and 62% in the RB10 segment, respectively.

Table 3
Pearson correlation coefficients between the CT measurements and airflow limitation.

	Generation	RB1	RB10
Mean-LA	3rd	0.08 (-0.11, 0.26)	0.08 (-0.11, 0.27)
	4th	0.18 (0.00, 0.36) *	0.14 (-0.05, 0.32)
	5th	0.37 (0.29, 0.52) **	0.23 (0.05, 0.40) *
	6th	0.32 (0.14, 0.48) **	0.16 (-0.03, 0.34)
Sum-LA	4th	0.16 (-0.03, 0.33)	0.15 (-0.04, 0.33)
	5th	0.32 (0.14, 0.48) **	0.31(0.13, 0.47) **
	6th	0.45 (0.29, 0.59) **	0.36 (0.18, 0.51) **
Number of Airways	5th	−0.09 (-0.27, 0.10)	0.19 (0.00, 0.37) *
	6th	0.27 (0.08, 0.43) **	0.33 (0.16, 0.49) **

Mean lumen area (Mean-LA) and sum of lumen areas (Sum-LA) of each generation in right apical bronchus and posterior basal bronchus segments (RB1 and RB10) were calculated. Values are the Pearson correlation coefficients (95% confidence interval) between percent of predicted forced expiratory volume in one second (%FEV_1) and CT measures. * and ** indicate $p < 0.05$ and $p < 0.01$, respectively.

[3,4]. Furthermore, the finding that U-HRCT failed to visualize the lumen of a phantom tube 0.5 mm in diameter (Fig. 1) suggests that the decrease in 6th generation airways in COPD might be because the 6th generation may include extremely small airways < 0.5 mm in diameter or because those airways do not actually exist.

In addition to the mean-LA, we measured the sum-LA to incorporate the effects of changes in the number of measurable airways of RB1 and RB10 segments in the luminal narrowing assessment. Consequently, among the correlations between FEV_1 and the mean and sum-LA, the sum-LA of the 6th generation airways had the greatest correlation coefficients. Moreover, the multivariable linear regression analyses showed that the sum-LA in the 6th generation airways of both the RB1 and RB10 segments were associated with %FEV_1 independent of LAV%. These findings suggest that the sum-LA of the 6th generation airways can be a promising CT biomarker that sensitively reflects airflow in COPD. Moreover, the finding that the association between the sum-LA and FEV_1 was stronger in the 6th generation than in the 4th and 5th generations supports the hypothesis that small airways more strongly contribute to airflow limitation in COPD than large airways [31,32].

Unlike the sum-LA, the associations between the mean-LA and FEV_1 were not greater in the 6th generation than in the 5th generation. This result is not consistent with a previous report that showed that the mean-LA of the 6th generation was more strongly correlated with FEV_1 than with any of the 3rd to 5th generations [13]. In addition to the limited image resolution, this discrepancy can be explained by the different sampling methods since the previous study analysed selected airways and not all measurable airways.

This study used the iterative reconstruction method named FIRST. While the FIRST method takes approximately 30 min to generate all 1024 × 1024 matrix images at 0.25 mm slice thickness for the entire lung [17], the FIRST method helps improve the signal-to-noise ratio of the images [22]. Indeed, the present results showed that the images reconstructed using the FIRST method allows clear visualization and accurate quantitative evaluation of peripheral airways 1–2 mm in diameter.

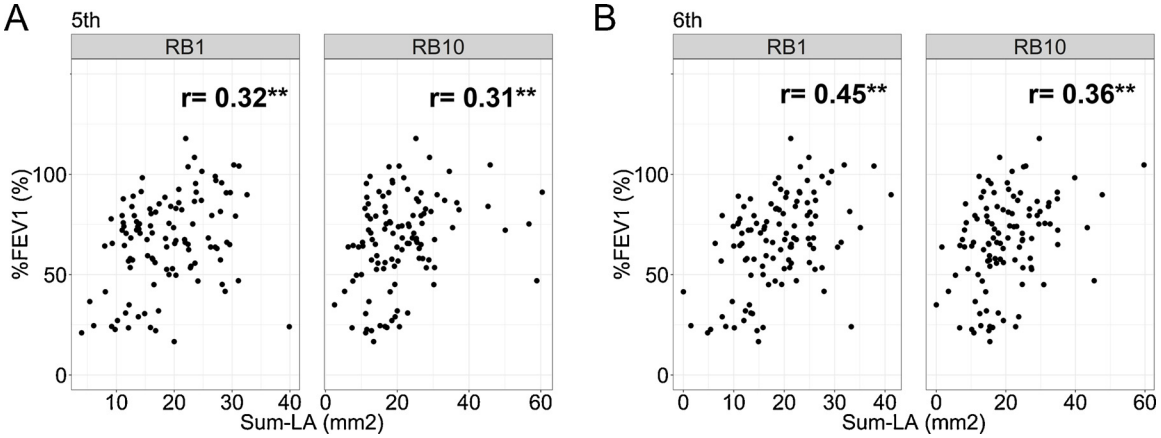

Fig. 5. Sum of lumen areas for the 5th and 6th generation airways and airflow limitation in COPD. RB1 and RB10 indicate the right apical and basal posterior segments, respectively. Sum-LA = sum of lumen areas. %FEV_1 = percent of predicted forced expiratory volume in one second. Total LA in the 5th (A) and 6th (B) generations was correlated with %FEV_1. The correlation between sum-LA and %FEV_1 was greater in the 6th generation than in the 5th generation. * and ** indicate $p < 0.05$ and $p < 0.01$, respectively.

Table 4
Multivariate linear regression analyses to explore the relative associations of luminal narrowing in the 6th generation airways and emphysema with airflow limitation.

Model 1	β (95%CI)	P value
Sum-LA (6th generation RB1 airways)	0.38 (0.23, 0.52)	< 0.001
LAV%	−0.51 (-0.66, -0.37)	< 0.001
Model 2	β (95%CI)	P value
Sum-LA (6th generation RB10 airways)	0.35 (0.21, 0.49)	< 0.001
LAV%	−0.56 (-0.71, -0.42)	< 0.001

Sum-LA = sum of lumen areas. RB1 = right apical bronchus segment. RB10 = right posterior basal bronchus segment. LAV% = low attenuation volume percent. 95%CI = 95% confidence interval. Each model included LAV% and sum-LA of the 6th generation airways in either the RB1 or RB10 as independent variables and percent of predicted forced expiratory volume in one second (% FEV_1) as a dependent variable. R-squared value (R^2) for model 1 and 2 were 0.45 and 0.44, respectively.

Some limitations need to be addressed. First, we confirmed the accuracy of measuring lumen size on U-HRCT using phantom tubes but not with the corresponding histology samples of human airways. Second, we did not include non−COPD healthy controls. We were not able to examine whether an airway < 2 mm in diameter could be found in the 6th generation, even in healthy controls. Third, we did not include females with COPD. It is unclear whether the present data can be applied to females with COPD. Fourth, because the iterative reconstruction potentially underestimates LAV% [33], the degree of emphysematous change on U-HRCT reconstructed using the FIRST method might be underestimated in this study.

In conclusion, the accurate computer-based U-HRCT quantitation of airways in patients with COPD revealed that the 6th generation airways in COPD are commonly < 2 mm in diameter and that the total cross-sectional lumen area of the 6th generation airways is a useful CT biomarker that reflects airflow limitation. The direct evaluation of peripheral airways 1–2 mm in diameter should be incorporated into a future study of COPD.

Declaration of Competing Interest

N.T., S.S, T.O. and T.H. were supported by a grant from FUJIFILM Co., Ltd.

K.T. was supported by Canon Medical Systems Corporation.

None of these companies had a role in the design or analysis of the study or in the writing of the manuscript.

Other authors have no conflict of interest to declare.

Acknowledgements

We would like to thank Aya Watanabe, Yoko Hamakawa, Kiyoshi Uemasu, and Tatsushi Mizutani for assistance with the data collection. This work was supported by grants from the Japan Society for the Promotion of Science (JSPS) [Grants-in-Aid for scientific research No. 17H06807 and No. 19K08624], Japan, and grants from FUJIFILM Co., Ltd, Japan and Canon Medical Systems Corporation, Japan.

Appendix A. Supplementary data

Supplementary material related to this article can be found, in the online version, at doi:https://doi.org/10.1016/j.ejrad.2019.108687.

References

[1] D. Adeloye, S. Chua, C. Lee, C. Basquill, A. Papana, E. Theodoratou, H. Nair, D. Gasevic, D. Sridhar, H. Campbell, K.Y. Chan, A. Sheikh, I. Rudan, G. Global health epidemiology reference, global and regional estimates of COPD prevalence: systematic review and meta-analysis, J. Glob. Health 5 (2) (2015) 020415.

[2] J.C. Hogg, Pathophysiology of airflow limitation in chronic obstructive pulmonary disease, Lancet 364 (9435) (2004) 709–721.

[3] H.K. Koo, D.M. Vasilescu, S. Booth, A. Hsieh, O.L. Katsamenis, N. Fishbane, W.M. Elliott, M. Kirby, P. Lackie, I. Sinclair, J.A. Warner, J.D. Cooper, H.O. Coxson, P.D. Pare, J.C. Hogg, T.L. Hackett, Small airways disease in mild and moderate chronic obstructive pulmonary disease: a cross-sectional study, Lancet Respir. Med. 6 (8) (2018) 591–602.

[4] J.E. McDonough, R. Yuan, M. Suzuki, N. Seyednejad, W.M. Elliott, P.G. Sanchez, A.C. Wright, W.B. Gefter, L. Litzky, H.O. Coxson, P.D. Pare, D.D. Sin, R.A. Pierce, J.C. Woods, A.M. McWilliams, J.R. Mayo, S.C. Lam, J.D. Cooper, J.C. Hogg, Small-airway obstruction and emphysema in chronic obstructive pulmonary disease, N. Engl. J. Med. 365 (17) (2011) 1567–1575.

[5] J.C. Hogg, F. Chu, S. Utokaparch, R. Woods, W.M. Elliott, L. Buzatu, R.M. Cherniack, R.M. Rogers, F.C. Sciurba, H.O. Coxson, P.D. Pare, The nature of small-airway obstruction in chronic obstructive pulmonary disease, N. Engl. J. Med. 350 (26) (2004) 2645–2653.

[6] N. Tanabe, D.M. Vasilescu, M. Kirby, H.O. Coxson, S.E. Verleden, B.M. Vanaudenaerde, D. Kinose, Y. Nakano, P.D. Pare, J.C. Hogg, Analysis of airway pathology in COPD using a combination of computed tomography, micro-computed tomography and histology, Eur. Respir. J. 51 (2) (2018).

[7] M. Saetta, W.D. Kim, J.L. Izquierdo, H. Ghezzo, M.G. Cosio, Extent of centrilobular and panacinar emphysema in smokers' lungs: pathological and mechanical implications, Eur. Respir. J. 7 (4) (1994) 664–671.

[8] M.K. Han, E.A. Kazerooni, D.A. Lynch, L.X. Liu, S. Murray, J.L. Curtis, G.J. Criner, V. Kim, R.P. Bowler, N.A. Hanania, A.R. Anzueto, B.J. Make, J.E. Hokanson, J.D. Crapo, E.K. Silverman, F.J. Martinez, G.R. Washko, C.O. Investigators, Chronic obstructive pulmonary disease exacerbations in the COPDGene study: associated radiologic phenotypes, Radiology 261 (1) (2011) 274–282.

[9] Y. Nakano, S. Muro, H. Sakai, T. Hirai, K. Chin, M. Tsukino, K. Nishimura, H. Itoh, P.D. Pare, J.C. Hogg, M. Mishima, Computed tomographic measurements of airway dimensions and emphysema in smokers. Correlation with lung function, Am. J.

Respir. Crit. Care Med. 162 (3 Pt 1) (2000) 1102–1108.
[10] T. Oguma, T. Hirai, A. Niimi, H. Matsumoto, S. Muro, M. Shigematsu, T. Nishimura, Y. Kubo, M. Mishima, Limitations of airway dimension measurement on images obtained using multi-detector row computed tomography, PLoS One 8 (10) (2013) e76381.
[11] B.M. Smith, E.A. Hoffman, D. Rabinowitz, E. Bleecker, S. Christenson, D. Couper, K.M. Donohue, M.K. Han, N.N. Hansel, R.E. Kanner, E. Kleerup, S. Rennard, R.G. Barr, Comparison of spatially matched airways reveals thinner airway walls in COPD. The Multi-Ethnic Study of Atherosclerosis (MESA) COPD Study and the Subpopulations and Intermediate Outcomes in COPD Study (SPIROMICS), Thorax 69 (11) (2014) 987–996.
[12] G.R. Washko, A.A. Diaz, V. Kim, R.G. Barr, M.T. Dransfield, J. Schroeder, J.J. Reilly, J.W. Ramsdell, A. McKenzie, E.J. Van Beek, D.A. Lynch, J.P. Butler, M.K. Han, Computed tomographic measures of airway morphology in smokers and never-smoking normals, J. Appl. Physiol. (1985) 116 (6) (2014) 668–673.
[13] M. Hasegawa, Y. Nasuhara, Y. Onodera, H. Makita, K. Nagai, S. Fuke, Y. Ito, T. Betsuyaku, M. Nishimura, Airflow limitation and airway dimensions in chronic obstructive pulmonary disease, Am. J. Respir. Crit. Care Med. 173 (12) (2006) 1309–1315.
[14] G. Mair, J. Maclay, J.J. Miller, D. McAllister, M. Connell, J.T. Murchison, W. MacNee, Airway dimensions in COPD: relationships with clinical variables, Respir. Med. 104 (11) (2010) 1683–1690.
[15] K. Shimizu, R. Seto, H. Makita, M. Suzuki, S. Konno, Y.M. Ito, R. Kanda, E. Ogawa, Y. Nakano, M. Nishimura, Computed tomography (CT)-assessed bronchodilation induced by inhaled indacaterol and glycopyrronium/indacaterol in COPD, Respir. Med. 119 (2016) 70–77.
[16] M. Kirby, N. Tanabe, W.C. Tan, G. Zhou, M. Obeidat, C.J. Hague, J. Leipsic, J. Bourbeau, D.D. Sin, J.C. Hogg, H.O. Coxson, C.C.R.G. Can, N. Canadian Respiratory Research, t.C.R.R.N. CanCold Collaborative Research Group, Total airway count on computed tomography and the risk of chronic obstructive pulmonary disease progression. Findings from a population-based study, Am. J. Respir. Crit. Care Med. 197 (1) (2018) 56–65.
[17] N. Tanabe, T. Oguma, S. Sato, T. Kubo, S. Kozawa, H. Shima, K. Koizumi, A. Sato, S. Muro, K. Togashi, T. Hirai, Quantitative measurement of airway dimensions using ultra-high resolution computed tomography, Respir. Investig. 56 (6) (2018) 489–496.
[18] A. Hata, M. Yanagawa, O. Honda, N. Kikuchi, T. Miyata, S. Tsukagoshi, A. Uranishi, N. Tomiyama, Effect of Matrix Size on the Image Quality of Ultra-high-resolution CT of the Lung: comparison of 512 x 512, 1024 x 1024, and 2048 x 2048, Acad. Radiol. (2018).
[19] M. Yanagawa, A. Hata, O. Honda, N. Kikuchi, T. Miyata, A. Uranishi, S. Tsukagoshi, N. Tomiyama, Subjective and objective comparisons of image quality between ultra-high-resolution CT and conventional area detector CT in phantoms and cadaveric human lungs, Eur. Radiol. 28 (12) (2018) 5060–5068.
[20] H. Takagi, R. Tanaka, K. Nagata, R. Ninomiya, K. Arakita, J.D. Schuijf, K. Yoshioka, Diagnostic performance of coronary CT angiography with ultra-high-resolution CT: comparison with invasive coronary angiography, Eur. J. Radiol. 101 (2018) 30–37.
[21] C.F. Vogelmeier, G.J. Criner, F.J. Martinez, A. Anzueto, P.J. Barnes, J. Bourbeau, B.R. Celli, R. Chen, M. Decramer, L.M. Fabbri, P. Frith, D.M. Halpin, M.V. Lopez Varela, M. Nishimura, N. Roche, R. Rodriguez-Roisin, D.D. Sin, D. Singh, R. Stockley, J. Vestbo, J.A. Wedzicha, A. Agusti, Global strategy for the diagnosis, management, and prevention of chronic obstructive lung disease 2017 report: GOLD executive summary, Eur. Respir. J. 49 (3) (2017).
[22] Y. Nishiyama, K. Tada, Y. Nishiyama, H. Mori, M. Maruyama, T. Katsube, N. Yamamoto, H. Kanayama, Y. Yamamoto, H. Kitagaki, Effect of the forward-projected model-based iterative reconstruction solution algorithm on image quality and radiation dose in pediatric cardiac computed tomography, Pediatr. Radiol. 46 (12) (2016) 1663–1670.
[23] K. Nishimoto, M. Karayama, N. Inui, K. Mori, M. Kono, H. Hozumi, Y. Suzuki, K. Furuhashi, N. Enomoto, T. Fujisawa, Y. Nakamura, H. Watanabe, T. Suda, Relationship between fraction of exhaled nitric oxide and airway morphology assessed by three-dimensional CT analysis in asthma, Sci. Rep. 7 (1) (2017) 10187.
[24] P.A. Gevenois, P. De Vuyst, V. de Maertelaer, J. Zanen, D. Jacobovitz, M.G. Cosio, J.C. Yernault, Comparison of computed density and microscopic morphometry in pulmonary emphysema, Am. J. Respir. Crit. Care Med. 154 (1) (1996) 187–192.
[25] M. Kubota, H. Kobayashi, P.H. Quanjer, H. Omori, K. Tatsumi, M. Kanazawa, S. Clinical Pulmonary Functions Committee of the Japanese Respiratory, Reference values for spirometry, including vital capacity, in Japanese adults calculated with the LMS method and compared with previous values, Respir. Investig. 52 (4) (2014) 242–250.
[26] J.M. Bland, D.G. Altman, Measurement error and correlation coefficients, BMJ 313 (7048) (1996) 41–42.
[27] J.M. Bland, D.G. Altman, Statistical methods for assessing agreement between two methods of clinical measurement, Lancet 1 (8476) (1986) 307–310.
[28] F.J. Martinez, J.L. Curtis, F. Sciurba, J. Mumford, N.D. Giardino, G. Weinmann, E. Kazerooni, S. Murray, G.J. Criner, D.D. Sin, J. Hogg, A.L. Ries, M. Han, A.P. Fishman, B. Make, E.A. Hoffman, Z. Mohsenifar, R. Wise, G. National Emphysema Treatment Trial Research, sex differences in severe pulmonary emphysema, Am. J. Respir. Crit. Care Med. 176 (3) (2007) 243–252.
[29] A. Tam, A. Churg, J.L. Wright, S. Zhou, M. Kirby, H.O. Coxson, S. Lam, S.F. Man, D.D. Sin, Sex differences in airway remodeling in a mouse model of chronic obstructive pulmonary disease, Am. J. Respir. Crit. Care Med. 193 (8) (2016) 825–834.
[30] A.A. Diaz, C. Valim, T. Yamashiro, R.S. Estepar, J.C. Ross, S. Matsuoka, B. Bartholmai, H. Hatabu, E.K. Silverman, G.R. Washko, Airway count and emphysema assessed by chest CT imaging predicts clinical outcome in smokers, Chest 138 (4) (2010) 880–887.
[31] J.C. Hogg, P.D. Pare, T.L. Hackett, The contribution of small airway obstruction to the pathogenesis of chronic obstructive pulmonary disease, Physiol. Rev. 97 (2) (2017) 529–552.
[32] J.C. Hogg, P.T. Macklem, W.M. Thurlbeck, Site and nature of airway obstruction in chronic obstructive lung disease, N. Engl. J. Med. 278 (25) (1968) 1355–1360.
[33] O.M. Mets, M.J. Willemink, F.P. de Kort, C.P. Mol, T. Leiner, M. Oudkerk, M. Prokop, P.A. de Jong, The effect of iterative reconstruction on computed tomography assessment of emphysema, air trapping and airway dimensions, Eur. Radiol. 22 (10) (2012) 2103–2109.